

Characterisation of gallium(III)-acetate complexes in aqueous solution: A potentiometric, EXAFS, IR and molecular orbital modelling study

Maria Clausén,^a Lars-Olof Öhman,^a James D. Kubicki^b and Per Persson^{*a}

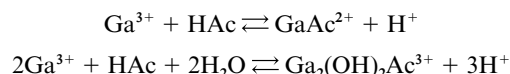
^a Department of Chemistry, Inorganic Chemistry, Umeå University, SE-901 87 Umeå, Sweden

^b Department of Geosciences, The Pennsylvania State University, University Park, PA 16802, USA

Received 18th December 2001, Accepted 10th April 2002

First published as an Advance Article on the web 8th May 2002

The aqueous gallium(III)-acetate system was studied in 0.6 M NaCl at 25 °C using a multi-technique approach, including potentiometry, IR spectroscopy, EXAFS spectroscopy and molecular orbital calculations. The potentiometric data were satisfactorily explained by a model which includes one mononuclear and one binuclear complex. The corresponding equilibrium constants defined according to the reactions



are $\log \beta_{-1,1,1} = -2.08 \pm 0.09$ and $\log \beta_{-3,2,1} = -5.65 \pm 0.06$, respectively. The latter complex has a stoichiometry identical to that previously identified in the aluminium(III)-acetate system. Also in agreement with this system, the IR and EXAFS data strongly indicates that this complex consists of two edge-sharing Ga octahedra bridged with an acetate ion, and should be formulated $[\text{Ga}_2(\mu\text{-OH})_2(\mu\text{-O}_2\text{CCH}_3)]^{3+}$. This interpretation is further supported by the molecular orbital calculations.

Introduction

The chemical speciation of metals (*i.e.*, the chemical form in terms of composition and structure) in the environment is fundamental to the understanding of reactivity, transport and bioavailability.¹ Since most reactions involving metals in the environment occur in aqueous solution or at water–solid interfaces it is of great importance to characterise *in-situ* metal speciation in aqueous solution. The present work concerns the Ga(III)-acetate system, and the main motivation for this study is as a comparison with the chemically related Al(III)-acetate system. Because of its geochemical significance Al(III)-acetate has been frequently studied, and two principally different chemical speciation models have been proposed.^{2,3} One model suggests the formation of mononuclear $[\text{Al}(\text{O}_2\text{CCH}_3)_x]^{3-x}$ complexes,² while the other involves the formation of a binuclear $[\text{Al}_2(\mu\text{-OH})_2(\mu\text{-O}_2\text{CCH}_3)]^{3+}$ complex.³ In a recent study, IR spectroscopic results were reported which were in excellent agreement with the latter model.⁴ However, no direct structural parameters (such as bond distances) for this complex have been presented. One of the few techniques capable of characterising dilute aqueous solutions is synchrotron-based EXAFS spectroscopy. Due to the low Al K edge energy (1.56 keV), however, the conventional EXAFS technique does not lend itself to studies of aqueous aluminium solutions. In contrast, the Ga K edge energy of 10.367 keV makes gallium a very suitable element for such studies. Thus, the aim of the present study has been to use a multi-technique approach including EXAFS to characterise the Ga(III)-acetate system and to compare the results with Al(III)-acetate. Stoichiometric compositions of appearing complexes were determined from potentiometry, while IR spectroscopy, EXAFS, and molecular orbital calculations were used to gain a structural insight into the complexes formed. Apart

from EXAFS, the other techniques have also been used previously in studies of Al(III)-acetate.^{2–5} As will be shown, Ga(III)-acetate behaves similarly to Al(III)-acetate, and the presence of a binuclear structure with a bridging acetate ion is strongly supported.

Experimental

Chemicals and solutions

Solutions of dilute HCl were prepared from concentrated hydrochloric acid (Fisher Chemicals, p.a.) and were standardised using tris(hydroxymethyl)aminomethane, “trisma-base” (Sigma p.a.), dried at 80 °C. Dilute, carbonate free, sodium hydroxide solutions were prepared from filtrated 50% NaOH (Merck, p.a.) and standardised against hydrochloric acid prepared as above. A stock solution of acetic acid (HAc) was prepared from glacial acetic acid (Merck, p.a.), and the acetate concentration was determined potentiometrically using the Gran extrapolation method.⁶ A stock solution of Ga(III) was prepared by dissolving $\text{Ga}(\text{NO}_3)_3 \cdot \text{H}_2\text{O}$ (Aldrich, 99.9%) in standardised hydrochloric acid, in order to prevent hydrolysis of the metal ion. The concentration of gallium was determined by indirect EDTA–Pb(NO₃)₂ titration, using xylenol orange as the indicator. All solutions were prepared in a medium of 0.6 M NaCl, using dried NaCl (Riedel-de Haën, p.a., 180 °C) and boiled deionized (Milli-Q 185 Plus) water.

The compositions of the solutions used for the EXAFS and IR experiments are summarised in Table 1. These compositions were chosen on the basis of extensive chemical modelling using the thermodynamic model presented herein. One objective with the calculations was to find solution conditions where Ga(III) hydrolysis products could be avoided. Except for the solution

Table 1 Solution concentrations and measured $-\log[\text{H}^+]$ values

	[Ga] _{tot} /mM	[Ac] _{tot} /mM	$-\log[\text{H}^+]$
IR			
a	80	40	1.04
b	80	40	1.74
c	80	40	1.85
d	80	40	2.00
e	80	40	2.10
f	80	40	2.24
g	80	40	2.36
h	80	40	2.47
i	80	40	2.54
j	80	40	2.58
k(D ₂ O)	80	40	2.43
EXAFS			
A	40	0	In conc. HNO ₃
B	40	440	2.34
C	40	440	2.49
D	40	440	2.63

denoted k(D₂O), they were all prepared from a stock solution of GaCl₃ (Aldrich, 99.999%), weighed amounts of sodium acetate (NaAc) (Riedel-de Haën, p.a.) and dried NaCl (Riedel-de Haën, p.a.). To reach different $-\log[\text{H}^+]$, appropriate amounts of dilute HCl or NaOH was added. The k(D₂O) solution was prepared from 99.9% D₂O (Sigma) and weighed amounts of anhydrous NaAc (Riedel-de Haën, p.a.), dried NaCl and Ga(NO₃)₃·H₂O (Aldrich, 99.9%). All solutions were prepared to contain 0.6 M NaCl, and they were left to equilibrate for at least 24 h before analysis. Beyond that time, $-\log[\text{H}^+]$ and IR spectra did not change and the solutions were considered stable. A combination glass electrode calibrated against a series of dilute hydrochloric acids in 0.6 M NaCl was used to measure $-\log[\text{H}^+]$.

Methods and measurements

Potentiometric titrations. The titrations were performed in a constant ionic medium of 0.6 M NaCl and at a temperature of 25 ± 0.1 °C. To prevent contamination from the atmosphere, moisturised argon gas was allowed to flow over the solutions during the entire data collection. The glass electrode set-up was calibrated at the beginning of each titration, *via* a step-wise coulometric neutralisation of HCl of known concentration, in 0.6 M NaCl, and the acetic acid and/or the Ga(III) solutions were then volumetrically added to this solution. The H⁺-acetic acid system has been previously studied in the same medium by Marklund *et al.*,³ and their acidity constant was shown to be in full agreement with our data. The H⁺-Ga³⁺ system was studied in a separate series of coulometric titrations consisting of three sets and 107 data points. The concentration of Ga(III) was varied between 3.96 and 11.48 mM and $2.2 \leq -\log[\text{H}^+] \leq 3.1$.

In the H⁺-acetic acid and H⁺-Ga³⁺-acetic acid systems, a dilute sodium hydroxide solution replaced the use of the coulometer to increase $-\log[\text{H}^+]$. This was due to an unwanted side reaction, possibly reduction of the ligand, which took place when the coulometer was used. Nine data sets, with a total of 128 data points, were used to determine the speciation in the three-component system. The initial concentrations were varied within the ranges $4.10 \leq [\text{HAc}]_{\text{tot}} \leq 28.83$ mM, $5.13 \leq [\text{Ga}^{3+}]_{\text{tot}} \leq 15.97$ mM and $2.1 \leq -\log[\text{H}^+] \leq 2.9$. The ratios between HAc and Ga(III) studied were 0.27, 0.44, 0.49, 0.62, 0.97, 1.04, 1.11, 1.48 and 4.16.

The upper $-\log[\text{H}^+]$ -limit in the titrations was determined by the on-set of extremely sluggish reactions, which has been interpreted as being due to the formation of a large polymer [Ga₁₃O₄(OH)₂₄(H₂O)₁₂]⁷⁺.^{7,8} All searches for the compositions of the complexes formed and optimisations were made using the LAKE computer program.⁹

IR spectroscopy. Attenuated Total Reflectance (ATR) IR spectra were collected using a Perkin-Elmer 2000 FTIR spectrometer fitted with a deuterated triglycine sulfate (DTGS) detector. The spectra were recorded with a horizontal ATR accessory with a diamond crystal as the reflection element (SensIR Technologies). The sample cell was purged with nitrogen gas throughout data collection to exclude carbon dioxide and water vapour. The angle of incidence for the set-up is approximately 45°, which is far from the critical angle. This and the fact that the bands analysed are weak (<0.05 absorbance units), and do not overlap with stronger bands (except for the asymmetric C–O stretch which overlaps with the intense H₂O bend), indicates that the effects of possible distortions known to occur in ATR spectra are minimised. The solutions were applied to the diamond crystal surface directly and a quartz lid was placed over the sample and pressed tightly against a rubber gasket. This sealed the sample from the atmosphere during data collection. 100 scans were collected for each sample over the range 370 to 7800 cm⁻¹ at a resolution of 4 cm⁻¹. The sample spectra were interpreted after subtracting spectra of both the empty cell and either H₂O or a combination of D₂O and HDO. The background solutions were all 0.6 M in NaCl.

EXAFS measurements. Ga K edge EXAFS data were measured at the Stanford Synchrotron Radiation Laboratory, California, on beam line 4–1. The ring energy was 3.0 GeV with ring currents between 60 and 100 mA. A Si(220) double crystal monochromator was used and detuned 50% to eliminate higher order harmonics. The data were collected at room temperature in the fluorescence mode, with a Lytle detector filled with Ar gas. A Zn filter and Soller slit set-up were used to reduce K_β fluorescence and scattering contributions to the signal. Internal calibration was performed by simultaneously measuring spectra from a Ga(OH)₃ reference sample in transmission mode, throughout the duration of all scans. Three to four scans were collected per sample.

EXAFS data treatment. The EXAFS data were energy-calibrated and averaged with EXAFSPAK,¹⁰ and further analysed using WinXAS.¹¹ Standard procedures were used for pre-edge subtraction, data normalisation, and spline removal. The *k*³-weighted EXAFS oscillations were Fourier transformed over the *k*-range 3.3–14.5 Å⁻¹ using a Kaiser–Bessel window function. Theoretical phase and amplitude functions for single and multiple scattering within assumed molecular models were calculated with the *ab initio* code FEFF7.¹² The gallium-acetate core of the crystal structure of di-μ-hydroxo-μ-acetato-bis-[(1,4,7-triazacyclononan)gallium(III)]triodide monohydrate¹³ was used as a model in the FEFF7 calculations for a bridging structure. The EXAFS spectrum of an acidic solution of gallium nitrate, where the Ga–O coordination number of Ga(H₂O)₆³⁺ is known to be six,¹⁴ was used to refine the amplitude reduction factor, *S*₀². This value was found to be 1.04, and was kept constant during the refinements of the gallium-acetate EXAFS spectra.

Molecular orbital calculations. Calculations were performed with the program Gaussian 98.¹⁵ Energy minimizations were conducted with internal redundant coordinates¹⁶ without any structural or symmetry constraints. The HF/3–21G(d,p) basis set¹⁷ was employed to model the electron density of the [Ga₂-(μ-OH)₂(μ-O₂CCH₃)(H₂O)₆·14H₂O]³⁺ cluster. Thus, to account for solvation effects explicit water molecules were included. This results in a cluster with a large number of atoms and, to limit the computational cost, a comparatively small basis set was used. As a consequence of this small basis set, the computed energies possibly have significant errors. Nevertheless, a good agreement is found between the computed properties (distances and frequencies) and experimental data (see Results and discussion). Furthermore, this computational approach

Table 2 Complexes in the H^+ – Ga^{3+} –acetic acid system. All the equilibria are written in the form $p\text{H}^+ + q\text{Ga}^{3+} + r\text{HAc} \rightleftharpoons \text{H}_p\text{Ga}_q(\text{HAc})_r^{(p+3q)}$

Reaction	$\log \beta_{p,q,r} \pm 3\sigma$	Ref.
$\text{H}_2\text{O} \rightleftharpoons \text{H}^+ + \text{OH}^-$	$\log \beta_{-1,0,0} = -13.73$	20
$\text{HAc} \rightleftharpoons \text{Ac}^- + \text{H}^+$	$\log \beta_{-1,0,1} = -4.49$	3
$\text{Ga}^{3+} + \text{H}_2\text{O} \rightleftharpoons \text{GaOH}^{2+} + \text{H}^+$	$\log \beta_{-1,1,0} = -4.02 \pm 0.08$	This work
$13\text{Ga}^{3+} + 32 \text{H}_2\text{O} \rightleftharpoons \text{Ga}_{13}(\text{OH})_{32}^{7+} + 32 \text{H}^+$	$\log \beta_{-32,13,0} = -67.14 \pm 0.06$	This work
$\text{Ga}^{3+} + \text{HAc} \rightleftharpoons \text{GaAc}^{2+} + \text{H}^+$	$\log \beta_{-1,1,1} = -2.08 \pm 0.09$	This work
$2\text{Ga}^{3+} + \text{HAc} + 2\text{H}_2\text{O} \rightleftharpoons \text{Ga}_2(\text{OH})_2\text{Ac}^{3+} + 3\text{H}^+$	$\log \beta_{-3,2,1} = -5.65 \pm 0.06$	This work

has been shown to be successful in modelling similar systems.¹⁸ Frequencies were scaled by 0.93, which was determined by comparing calculated frequencies of C–O modes in $[\text{CH}_3\text{CO}_2^-] \cdot 14(\text{H}_2\text{O})$ with experimentally observed values of acetate in aqueous solution.

Results and discussion

Potentiometry and equilibrium model

The H^+ – Ga^{3+} system. Data in the current concentration and $-\log[\text{H}^+]$ range could be explained by the formation of one mononuclear complex $\text{Ga}(\text{OH})^{2+}$ and one large polymeric species $\text{Ga}_{13}(\text{OH})_{32}^{7+}$. This is in accordance with the present view on the hydrolysis of $\text{Ga}(\text{III})$.^{7,8,19} The equilibrium constants resulting from the refinements are given in Table 2.

The H^+ – Ga^{3+} – HAc system. In the evaluation of the ternary system, the equilibrium constants for the binary systems were considered known and were kept constant. The stoichiometry of the three-component species offering the closest fit to experimental data was evaluated by using the so-called (p,q,r) -analysis technique.²¹ In this technique, all relevant integer values of $\text{H}_p\text{Ga}_q(\text{HAc})_r^{p+3q}$ are tested, one by one, by optimising the equilibrium constant and recording the resulting error sum of squares, $U = \sum (H_{\text{calc}} - H_{\text{exp}})^2$. The result of this search is illustrated in Fig. 1 and shows that the single complex best

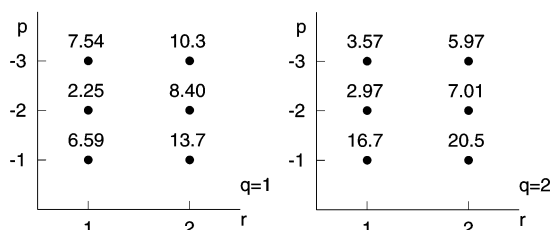


Fig. 1 Results of the (p,q,r) -analysis on data in the H^+ – Ga^{3+} – HAc system. One ternary complex is assumed, with the “best possible” equilibrium constant, and the figure gives the error sum of squares $10^6 U_{\text{H}(pr)}_q$ for each (p,q,r) composition.

describing the data is $\text{H}_2\text{Ga}(\text{HAc})^+$ (with $\log \beta_{-2,1,1} = -4.67 \pm 0.03$). Also with this complex, however, systematic residuals appeared in the data material, and imply that the stoichiometry indicated represents an average only.

We therefore expanded our search to include a combination of two simultaneously forming complexes, and with an average of approximately $\text{H}_2\text{Ga}(\text{HAc})$. The combinations tested were $\text{H}_1\text{Ga}(\text{HAc}) + \text{H}_2\text{Ga}(\text{HAc})$, $\text{H}_1\text{Ga}(\text{HAc}) + \text{H}_3\text{Ga}(\text{HAc})$, $\text{H}_1\text{Ga}(\text{HAc}) + \text{H}_2\text{Ga}_2(\text{HAc})$, $\text{H}_1\text{Ga}(\text{HAc}) + \text{H}_3\text{Ga}_2(\text{HAc})$, $\text{H}_2\text{Ga}(\text{HAc}) + \text{H}_2\text{Ga}_2(\text{HAc})$, and $\text{H}_2\text{Ga}(\text{HAc}) + \text{H}_3\text{Ga}_2(\text{HAc})$. The combination $\text{H}_1\text{Ga}(\text{HAc}) + \text{H}_3\text{Ga}_2(\text{HAc})$ was found to yield the best fit to data ($U = 1.48 \times 10^{-6}$, $\sigma(\text{H}) = 0.078 \times 10^{-3} \text{ M}$) and no systematic behaviour in the remaining residuals could be discerned. The optimised equilibrium constants and corresponding standard deviations are presented in Table 2.

Thus, one of the complexes identified was found to carry the same stoichiometry as the complex identified in the related aluminium(III)-acetate system,³ $\text{H}_3\text{Al}_2(\text{HAc})^{3+}$, and the second

species is a simple GaAc^{2+} complex. Although it is difficult to certify the absolute uniqueness of this model, it will be shown that the model is corroborated by the good agreement with the spectroscopic and theoretical results presented below.

IR spectroscopy

Identification of gallium(III)-acetate complexes. The IR spectra of solutions a–j (*cf.* Table 1) can conceivably contain signals from acetic acid, acetate ions, and $\text{Ga}(\text{III})$ -acetate complexes. According to the thermodynamic model presented above, contributions from acetic acid and two $\text{Ga}(\text{III})$ -acetate complexes are to be expected; the acetate concentration under the experimental conditions studied is predicted to be too low for detection. A selection of spectra show that acetic acid and one $\text{Ga}(\text{III})$ -acetate complex are readily detected (Fig. 2). Acetic

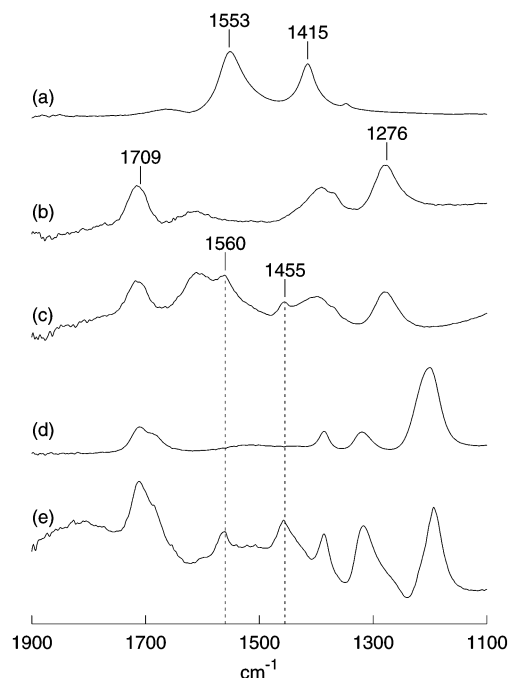


Fig. 2 Attenuated total reflectance FTIR spectra of (a) 0.170 M sodium acetate, (b) 0.040 M acetic acid, (c) an aqueous solution containing $[\text{Ga}^{3+}]_{\text{tot}} = 0.080 \text{ M}$ and $[\text{HAc}]_{\text{tot}} = 0.040 \text{ M}$ at $-\log[\text{H}^+] = 2.47$, (d) deuterated solution containing $[\text{Dac}] = 0.040 \text{ M}$ (e) deuterated solution containing $[\text{Ga}^{3+}]_{\text{tot}} = 0.080 \text{ M}$ and $[\text{Dac}]_{\text{tot}} = 0.040 \text{ M}$ at $\text{pD} = 2.43$. All the solutions were prepared in 0.6 M NaCl. The ordinate scale is in absorbance units and is arbitrary.

acid is characterised by bands at 1709 and 1276 cm^{-1} , which originate from the $\nu_{\text{C-O}}$ and $\nu_{\text{C-OH}} + \delta_{\text{C-O-H}}$ modes, respectively.⁴ The $\text{Ga}(\text{III})$ -acetate complex displays two bands at 1560 and 1455 cm^{-1} (Fig. 2). In H_2O , a precise characterisation of the 1560 cm^{-1} band is made difficult due to a partial overlap with the strong $\delta_{\text{H}_2\text{O}}$ mode of bulk and coordinated water. In D_2O , however, both the 1560 and 1455 cm^{-1} bands are clearly resolved (Fig. 2). Note that these bands are significantly shifted from the asymmetric and symmetric $\nu_{\text{C-O}}$ of the acetate ion in aqueous solution at 1553 and 1415 cm^{-1} , respectively, which indicates that the acetate ion is directly coordinated to $\text{Ga}(\text{III})$ as an inner-sphere ligand (Fig. 2). The assignment and the struc-

tural implications will be discussed below. The bands at 1560 and 1455 cm^{-1} are also clearly visible in the spectra of all solutions used for the EXAFS experiments, thereby indicating that the same complex is studied in both experimental series.

The IR data can be used to quantify the species in solution and, in this way, be compared with the speciation predicted from the thermodynamic model. The acetic acid concentration can be followed by measuring changes in the area of the band at 1276 cm^{-1} . This band is preferred to the band at 1709 cm^{-1} , since it is less affected by the large absorption by water. Analyses of replica of the spectra, showed that this band area could be determined with a reproducibility of better than 3%. By using a 40.0 mM solution of HAc for a one-point determination of the molar absorptivity of the 1276 cm^{-1} band, the free acetic acid concentration could be quantified in all solutions studied. We found that its behaviour harmonised well with the behaviour predicted by the complexation model presented herein, as shown in Fig. 3a, but was in sharp contrast to a previ-

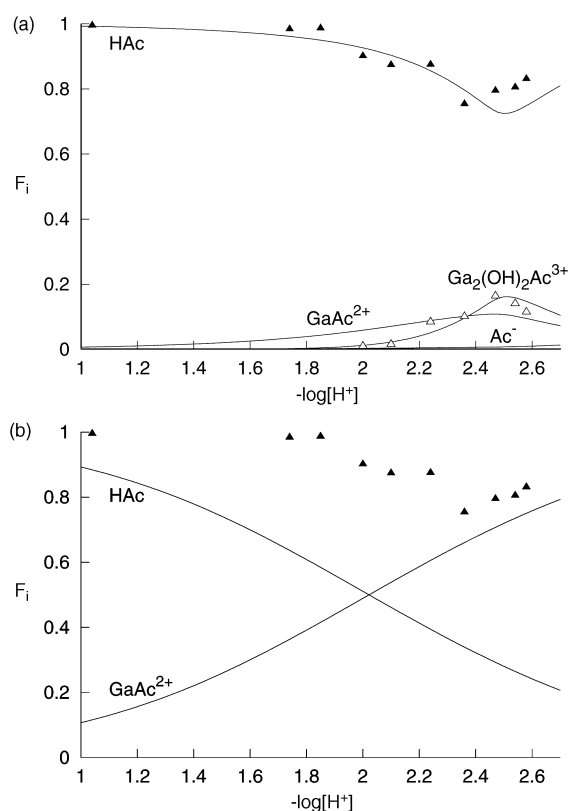


Fig. 3 Calculated distribution diagrams, $F_i(-\log[H^+])$, where F_i is the ratio between acetate in a species and the total acetate. The diagrams were constructed at $[\text{Ga}]_{\text{tot}} = 0.080 \text{ M}$ and $[\text{HAc}]_{\text{tot}} = 0.040 \text{ M}$ using (a) the equilibrium model presented in this paper and (b) the model presented by Skorik and Artish.²² The triangles represent the concentrations calculated from IR band areas of the 1276 cm^{-1} (▲, HAc) and 1455 cm^{-1} (Δ, $\text{H}_{-3}\text{Ga}_2(\text{HAc})^{3+}$) band as a function of $-\log[H^+]$, respectively.

ous model proposed by Skorik and Artish,²² in which a mononuclear complex was assumed to be the only complex formed (Fig. 3b).

Similarly, the concentration of the Ga(III)-acetate complex can be followed by analysis of the band area at 1455 cm^{-1} . When this band area is plotted as a function of $-\log[H^+]$, it is found that it follows the predicted concentration of the $\text{H}_{-3}\text{Ga}_2(\text{HAc})^{3+}$ complex. In Fig. 3a, the areas have been converted to concentrations through an estimation of the molar absorptivity by using the sample with the largest band area ($-\log[H^+] = 2.47$) and the concentration predicted by the model. As seen, a fair agreement is obtained between the concentrations estimated from the IR band areas and the poten-

tiometrically derived model. This suggests that the bands at 1560 and 1455 cm^{-1} originate from the binuclear complex. As will be shown below, this is also in agreement with the EXAFS results. Frequencies originating from the mononuclear complex could not be located with certainty in the spectra, probably due to a low concentration in combination with possible band overlap with the strong $\delta_{\text{H}_2\text{O}}$ mode of water and the HAc bands.

Acetate coordination mode and band assignments. Thus, the stoichiometry of the detected Ga(III)-acetate complex is indicated to be $\text{H}_{-3}\text{Ga}_2(\text{HAc})^{3+}$, and this complex is characterized by bands at 1560 and 1455 cm^{-1} . In analogy with the acetate ion, these bands are commonly assigned to the asymmetric ($\nu_{\text{C-O}^{\text{a}}}$) and the symmetric ($\nu_{\text{C-O}^{\text{s}}}$) stretching vibrations of the $-\text{CO}_2^-$ group, respectively. These frequencies and, in particular, the split between them have been used as empirical indicators of acetate coordination modes. According to Deacon and Phillips,²³ a split larger than 200 cm^{-1} indicates a monodentate coordination whereas a split smaller than 150 cm^{-1} indicates either a bridging or a chelating binding mode. These conclusions are also supported by theoretical calculations.⁵ The analogous complex $\text{H}_{-3}\text{Al}_2(\text{HAc})^{3+}$, previously identified by Marklund *et al.*,³ displays $\nu_{\text{C-O}^{\text{a}}}$ at 1581 cm^{-1} and $\nu_{\text{C-O}^{\text{s}}}$ at 1474 cm^{-1} , a split of 107 cm^{-1} .⁴ This split, and the shifts of $\nu_{\text{C-O}^{\text{a}}}$ and $\nu_{\text{C-O}^{\text{s}}}$ as compared to free acetate, was shown by Persson *et al.*⁴ to be indicative of acetate in a bridging coordination mode. The almost identical splitting in the present system, 105 as compared to 107 cm^{-1} , and the direction of the shifts of $\nu_{\text{C-O}^{\text{a}}}$ and $\nu_{\text{C-O}^{\text{s}}}$ in comparison with free acetate, indicates that the binuclear $\text{H}_{-3}\text{Ga}_2(\text{HAc})^{3+}$ complex also contains a bridging acetate ion.

Theoretical frequencies from molecular orbital calculations.

Throughout numerous calculations on carboxylate species, the general frequency correction factor of 0.893²⁴ has proven to give inaccurate results.²⁵ The original value may be in error in this case because modes involving anions and $\text{O} \cdots \text{O}$ interactions should not be expected to have the same error in basis set and electron correlation as neutral species involving only C and H. Hence, vibrational frequencies were calculated for the cluster $[\text{CH}_3\text{CO}_2^-] \cdot 14\text{H}_2\text{O}$ and compared to experimental frequencies. A scale factor of 0.93 is determined for both the $\nu_{\text{C-O}^{\text{s}}}$ and $\nu_{\text{C-O}^{\text{a}}}$ modes. Using this scale factor on vibrational frequencies calculated for the $\nu_{\text{C-O}^{\text{s}}}$ and $\nu_{\text{C-O}^{\text{a}}}$ modes in the $[\text{Ga}_2(\mu\text{-OH})_2(\mu\text{-O}_2\text{CCH}_3)(\text{H}_2\text{O})_6 \cdot 14\text{H}_2\text{O}]^{3+}$ cluster, gives frequencies of 1442 and 1471 cm^{-1} for the $\nu_{\text{C-O}^{\text{s}}}$ mode and 1560 cm^{-1} for the $\nu_{\text{C-O}^{\text{a}}}$ mode. These modes are also predicted to have the highest infrared intensities of any modes within the range 1000 to 2000 cm^{-1} . There is a perfect agreement between the experimental and theoretical frequency for $\nu_{\text{C-O}^{\text{a}}}$, while the average of the two $\nu_{\text{C-O}^{\text{s}}}$ modes is 1457 cm^{-1} , fortuitously close to the observed 1455 cm^{-1} value. Such agreement is suggestive, however, the results strongly indicate that the 1455 cm^{-1} mode is actually made up of two contributions. Modal analysis of the frequency calculation shows that the C–O stretches are mixed with distortion of the methyl group which gives rise to the separate theoretical frequencies at 1442 and 1471 cm^{-1} . In summary, the good agreement between experimental and theoretical frequencies further supports the existence of a bridging acetate ion.

EXAFS

The k^3 -weighted EXAFS spectra and the corresponding Fourier transforms of solutions B–D and of an acidic gallium nitrate solution, A, are displayed in Fig. 4. The latter solution is dominated by $[\text{Ga}(\text{H}_2\text{O})_6]^{3+}$, which has been shown previously to have the form of a regular octahedron with a Ga–O distance of 1.96 Å.¹⁴ The beat pattern around 4 Å⁻¹ is partly due to multiple scattering within the first coordination shell of six

Table 3 Results from *R*-space fits of EXAFS data

	Ga–O			Ga–Ga			$\Delta E_0/\text{eV}$
	Coord. no.	<i>R</i> /Å	σ^2	Coord. no. ^a	<i>R</i> /Å	σ^2	
B	5.8	1.960	0.0048	0.26	2.940	0.0055	1.6
C	5.9	1.960	0.0050	0.33	2.933	0.0057	1.5
D	5.9	1.960	0.0050	0.42	2.925	0.0056	1.8

^a Coordination numbers estimated from the extrapolated speciation model are 0.2, 0.3 and 0.4. Uncertainties in *R* are estimated in the 1st shell to ± 0.02 Å and in the 2nd shell to ± 0.03 Å. Uncertainties in coordination numbers are estimated to $\pm 20\%$.

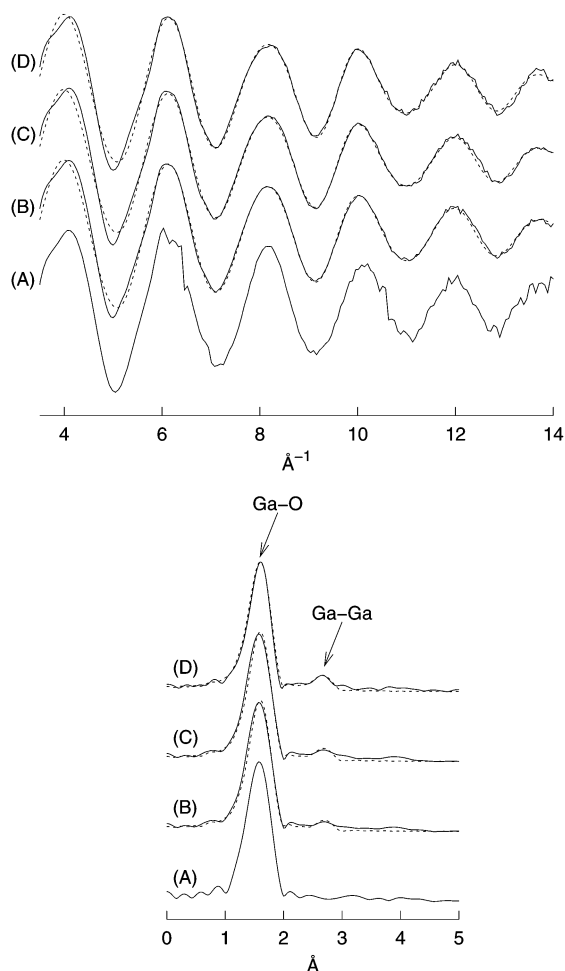


Fig. 4 k^3 -weighted EXAFS and the corresponding Fourier transforms of solutions containing $[\text{Ga}]_{\text{tot}} = 0.040$ M and $[\text{HAc}]_{\text{tot}} = 0.440$ M with (B) $-\log[\text{H}^+] = 2.34$, (C) $-\log[\text{H}^+] = 2.49$ and (D) $-\log[\text{H}^+] = 2.63$. The spectrum of an acidic aqueous solution of $\text{Ga}(\text{NO}_3)_3$ (A) is included for comparison. The Fourier transforms are uncorrected for phase shift. Dotted lines represent the models presented in Table 3.

oxygen atoms. Full multiple calculations with FEFF7 show that this feature is dominated by linear three-leg ($\text{O}_I\text{--Ga--O}_{II}$) and four-leg ($\text{O}_I\text{--Ga--O}_{II}\text{--Ga}$) scattering paths. Overall, the EXAFS data of the gallium-acetate solutions are similar to the EXAFS of $[\text{Ga}(\text{H}_2\text{O})_6]^{3+}$. However, as the $-\log[\text{H}^+]$ increases, a new second coordination shell appears in the Fourier transforms at 2.7 Å (uncorrected for phase shift). The appearance of this feature correlates to the appearance of the IR frequencies at 1560 and 1455 cm^{-1} discussed above.

Analysis of the first coordination shell. The multiple scattering contributions within the 1st coordination shell appear at the double single scattering distance, and a complete fit of these features results in a large number of fit variables. In order to keep the number of variables low, we have chosen not to include the multiple scattering contributions in the fit. This is accom-

plished by analysing Fourier transforms just past the second shell at 2.7 Å, which is significantly shorter than the multiple scattering distances. Thus, all results presented herein are obtained from *R*-space fits. The first shell is satisfactorily modelled by close to six oxygen neighbours at 1.96 Å (Table 3), which is in agreement with Ga(III) in an octahedral coordination geometry.¹⁴ No trends in the refined fit parameters are observed as a function of $-\log[\text{H}^+]$. Thus, the appearance of the second shell at 2.7 Å is not accompanied by detectable changes in the first shell EXAFS data.

Analysis of the second coordination shell. The envelope of the filtered EXAFS of the second shell peak indicates that back-scattering is caused by a heavy atom and, therefore, a Ga–Ga scattering pair is indicated. The fit reveals a gallium ion at 2.93 Å, with an increasing coordination number at increasing $-\log[\text{H}^+]$ (Table 3).

Predictions made by extrapolating the thermodynamic model to conditions in the EXAFS solutions show (*cf.* footnote to Table 3) that the concentration of $\text{H}_3\text{Ga}_2(\text{HAc})^{3+}$ is expected to increase in the solutions B through D. This is in agreement with the increase in Ga–Ga coordination number determined by EXAFS (Table 3). Furthermore, both the Ga–Ga coordination numbers and the thermodynamic predictions correlate with the intensities of the IR frequencies at 1560 and 1455 cm^{-1} . We thus conclude that the complex with the stoichiometry $\text{H}_3\text{Ga}_2(\text{HAc})^{3+}$ is characterized by a Ga–Ga distance of 2.93 Å and IR frequencies which are indicative of a bridging coordination of the acetate ion. Accordingly we suggest that this complex should be formulated as $[\text{Ga}_2(\mu\text{-OH})_2(\mu\text{-O}_2\text{-CCH}_3)]^{3+}$.

The hydrolysis of Ga(III) has been shown to yield polynuclear species with Ga–Ga distances of 3.05, 3.50, and 3.90 Å.²⁶ The shorter distance is indicative of edge-sharing gallium octahedra. Similar edge-sharing distances are observed in $\beta\text{-Ga}_2\text{O}_3$ (3.04 and 3.11 Å).²⁷ The distance observed in the present gallium-acetate complex is thus significantly shorter than typical edge-sharing distances of polynuclear $\text{Ga}_x\text{O}_y(\text{OH})_z$ solution complexes. This can be explained by the presence of the bridging acetate ion, where the coordination to the apices of the octahedra causes a tilt which reduces the Ga–Ga distance. Indeed, the crystal structure of di- μ -hydroxo- μ -acetato-bis-[(1,4,7-triazacyclononan)gallium(III)]triiodide monohydrate,¹³ which has been shown to contain this structural element, has a Ga–Ga distance of 2.927 Å, in very good agreement with the Ga–Ga distance determined herein. This structural interpretation is further supported by the optimised structure of $[\text{Ga}_2(\mu\text{-OH})_2(\mu\text{-O}_2\text{CCH}_3)(\text{H}_2\text{O})_6 \cdot 14\text{H}_2\text{O}]^{3+}$, which displays a Ga–Ga distance of 2.96 Å and a pronounced tilt of the Ga octahedra (Fig. 5). We therefore conclude that the significant shortening of the Ga–Ga distance, as compared to typical octahedral edge-sharing distances, support the existence of a bridging acetate ligand.

Acknowledgements

We would like to thank Mrs Agneta Nordin for help with the potentiometric measurements and Prof. Staffan Sjöberg for

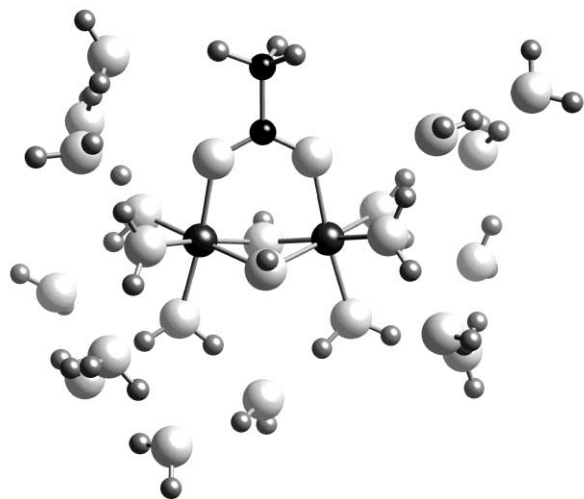


Fig. 5 Optimised structure from the molecular orbital calculations of $[\text{Ga}_2(\mu\text{-OH})_2(\mu\text{-O}_2\text{CCH}_3)(\text{H}_2\text{O})_6 \cdot 14\text{H}_2\text{O}]^{3+}$.

valuable suggestions and comments. Dr. Frank Wikström is acknowledged for his assistance with the illustrations. We thank the staff of Stanford Synchrotron Radiation Laboratory (SSRL), particularly Prof. Britt Hedman and Dr John Bargar, for their help and advise. SSRL is operated by the Department of Energy, Office of Basic Energy Sciences. We also acknowledge the National Institutes of Health, National Center for Research Resources, Biomedical Technology Program, and the Department of Energy Office of Biological and Environmental Research, which support the SSRL Structural Molecular Biology Program whose instrumentation was used for the measurements. This work was supported by the Swedish Research Council.

References

- 1 W. Stumm, *Chemistry of the Solid–Water Interface*, Wiley, New York, 1992.
- 2 D. A. Palmer and J. L. S. Bell, *Geochim. Cosmochim. Acta*, 1994, **58**, 651.
- 3 E. Marklund, L.-O. Öhman and S. Sjöberg, *Acta Chem. Scand.*, 1989, **43**, 641.
- 4 P. Persson, M. Karlsson and L.-O. Öhman, *Geochim. Cosmochim. Acta*, 1998, **62**, 3657.
- 5 J. D. Kubicki, G. A. Blake and S. E. Apitz, *Geochim. Cosmochim. Acta*, 1996, **60**, 4897.
- 6 C. Gran, *Acta Chem. Scand.*, 1950, **4**, 559.
- 7 S. M. Bradley, R. A. Kydd and R. Yamdagni, *J. Chem. Soc., Dalton Trans.*, 1990, 413.
- 8 S. M. Bradley, R. A. Kydd and R. Yamdagni, *J. Chem. Soc., Dalton Trans.*, 1990, 2653.
- 9 N. Ingri, I. Andersson, L. Pettersson, A. Yagasaki, L. Andersson and K. Holmström, *Acta Chem. Scand.*, 1996, **50**, 717.
- 10 G. N. George and I. J. Pickering, EXAFSPAK – A Suite of Computer Programs for Analysis of X-ray Absorption Spectra, SSRL, Stanford, CA, 1993.
- 11 T. Ressler, WinXAS software for EXAFS data reduction, 1998. See www.winxas.de.
- 12 S. I. Zabinsky, J. J. Rehr, A. Ankudinov, R. C. Albers and M. J. Eller, *Phys. Rev. B*, 1995, **52**, 2995.
- 13 K. Wieghardt, M. Kleine-Boymann, B. Nuber and J. Weiss, *Z. Anorg. Allg. Chem.*, 1986, **536**, 176.
- 14 P. Lindqvist-Reis, A. Muñoz-Páez, S. Díaz-Moreno, S. Pattanaik, I. Persson and M. Sandström, *Inorg. Chem.*, 1998, **37**, 6675.
- 15 M. J. Frisch, G. W. Trucks, H. B. Schlegel, P. M. W. Gill, B. G. Johnson, M. A. Robb, J. R. Cheeseman, T. Keith, G. A. Petersson, J. A. Montgomery, K. Raghavachari, M. A. Al-Laham, V. G. Zakrzewski, J. V. Ortiz, J. B. Foresman, J. Cioslowski, B. B. Stefanov, A. Nanayakkara, M. Chaloccombe, C. Y. Peng, P. Y. Ayala, W. Chen, M. W. Wong, J. L. Andres, E. S. Replogle, R. Comperts, R. L. Martin, D. J. Fox, J. S. Binkley, D. J. Defrees, J. Baker, J. P. Stewart, M. Head-Gordon, C. Gonzalez and J. A. Pople, Gaussian 98, Revision A.7, Gaussian, Inc., Pittsburgh, PA, 1998.
- 16 C. Peng, P. Y. Ayala, H. B. Schlegel and M. J. Frisch, *J. Comp. Chem.*, 1996, **17**, 49.
- 17 J. S. Binkley, J. A. Pople and W. J. Hehre, *J. Am. Chem. Soc.*, 1980, **102**, 939.
- 18 J. D. Kubicki and P. Persson, to be published.
- 19 C. F. Baes and R. E. Mesmer, in *The Hydrolysis of Cations*, R. E. Krieger, ed., Publishing Company, Malabar, Florida, 1986.
- 20 S. Sjöberg, A. Nordin and N. Ingri, *Mar. Chem.*, 1981, **10**, 521.
- 21 L.-O. Öhman and S. Sjöberg, *Coord. Chem. Rev.*, 1996, **149**, 33.
- 22 N. A. Skorik and A. S. Artish, *Russ. J. Inorg. Chem.*, 1985, **30**, 1130.
- 23 G. B. Deacon and R. J. Phillips, *Coord. Chem. Rev.*, 1980, **33**, 227.
- 24 J. A. Pople, H. B. Schlegel, R. Krishnan, D. J. Defrees, J. S. Binkley, M. J. Frisch, R. A. Whiteside, R. F. Hout and W. J. Hehre, *Int. J. Quantum Chem.: Quantum Chem. Symp.*, 1981, **15**, 269.
- 25 J. D. Kubicki, L. M. Schroeter, M. J. Itoh, B. N. Nguyen and S. E. Apitz, *Geochim. Cosmochim. Acta*, 1999, **63**, 2709.
- 26 L. J. Michot, E. Montargès-Pelletier, B. S. Lartiges, J.-B. despinose de la Caillerie and V. Briois, *J. Am. Chem. Soc.*, 2000, **122**, 6048.
- 27 S. Geller, *J. Chem. Phys.*, 1960, **33**, 676.